Structure of Carbon Dioxide Phase IV: Breakdown of the Intermediate Bonding State Scenario

Frédéric Datchi,[1,2] Valentina M. Giordano,[3] Pascal Munsch,[1,2] and A. Marco Saitta[1,2]
[1] *UPMC University of Paris 06, UMR 7590, IMPMC, F-75015 Paris, France*
[2] *CNRS, UMR 7590, IMPMC, F-75015 Paris, France*
[3] *European Radiation Synchrotron Facility, F-38043 Grenoble CEDEX, France*
(Received 9 July 2009; revised manuscript received 13 October 2009; published 29 October 2009)

The existence of "intermediate bonding states" in solid CO_2, separating the low-pressure molecular phases from the high-pressure polymeric forms, has been the matter of a long-standing debate. Here we determine the structure of CO_2-IV using x-ray diffraction of single crystals grown inside a diamond anvil cell at 11.7 GPa and 830 K. It is rhombohedral, space group $R\bar{3}c$, and is composed of individual, linear CO_2 molecules with bond lengths of 1.155(2) Å at 15 GPa. This shows that CO_2 remains a purely molecular solid in this P-T range, and thus invalidates the intermediate bonding state scenario. First-principles calculations confirm the stability of the proposed structure and match very well observations, including the Raman and IR spectra. Furthermore, these results evidence a striking similarity between the high-pressure polymorphs of solid CO_2 and N_2.

DOI: 10.1103/PhysRevLett.103.185701 PACS numbers: 64.70.kt, 07.35.+k, 61.50.Ks, 78.30.−j

The transformations of molecular crystals to new, nonmolecular phases at very high pressures have attracted a formidable interest in the recent past, motivated both by fundamental questions on the evolution of molecular bonds at high density, and by the prospects of creating novel materials with remarkable properties, such as superhardness, high T_c superconductivity or high energy density storage. The case of carbon dioxide has been granted particular attention since the discovery, at high P-T, of a crystalline, nonmolecular phase (CO2-V), with an experimental bulk modulus in the range of superhard solids [1,2]. X-ray diffraction data suggested that its structure is similar to tridymite SiO_2 ($P2_12_12_1$), with interconnected layers of tetrahedral CO_4 units [2]. There is still a debate on the actual structure of this phase but a general agreement on the presence of fourfold coordinated carbon (for a recent review, see Ref. [3]). More recently, two other nonmolecular phases have been reported [4,5], showing evidence of mixed threefold and fourfold coordinated carbon [6]. All these transformations thus involve the breaking of the double $C=O$ bond and the formation of new single bonds to produce an extended covalent solid.

The microscopic mechanisms underlying these transformations are still unknown. Two competing scenarios have been formulated: on the one hand, it has been assessed that the molecules gradually distort as P and T increase, going from the linear entity with $C=O$ distance of 1.168 Å stable at ambient, to a bent and strongly elongated form, and that this distortion acts as a seed to the formation of new bonds at higher T [7]. On the other hand, the transformation is considered as a true chemical reaction between neighboring molecules, occurring when intermolecular distances are short enough and the temperature high enough to initiate the reaction [8]. The first scenario has been mainly based on the structures proposed for the crystal phases II and IV present in the intermediate P-T range between the molecular phase I and extended phases (Fig. 1) [7,9]: the $C=O$ bond lengths showed an increase of 15% and 30%, respectively, for CO_2-II ($P4_2/mnm$) and IV ($Pbcn$), and the $O=C=O$ angle bent to 160° in phase IV. These two phases were thus designated as "intermediate bonding states" [5,7,9]. The second viewpoint stems from several pieces of evidence that phases II and IV are in fact purely molecular phases, coming either from theoretical calculations [10], spectroscopic data [8], or the discovery of another phase, VII, with a purely molecular character in the same P-T range as phases II and IV [11].

In this Letter we report direct experimental evidence that carbon dioxide remains a strictly molecular solid in the stability range of phase IV. We have succeeded in growing

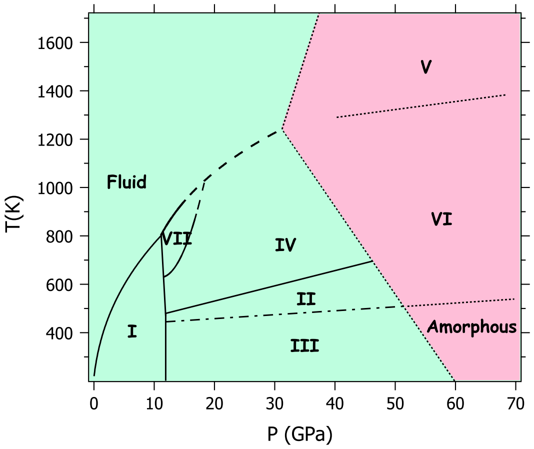

FIG. 1 (color online). Phase diagram of CO_2 at high P-T. The dashed lines show extrapolations of measurements, the dash-dotted line is thought to be a kinetic line, and dotted lines are hypothetic transition lines reproduced from Ref. [5]. Different colors distinguish molecular from nonmolecular phases.

single crystals of this phase and determined its structure using x-ray diffraction (XRD). The latter has no resemblance with the one proposed in Ref. [7] from refinement of powder XRD data. The most remarkable difference is that the molecules keep the shape typical of the isolated monomer.

The present experiments were performed on CO_2 samples loaded in a diamond anvil cell. The techniques employed here are identical to those described in detail in Ref. [12]. To grow a single crystal of phase IV, we used our previous observation that, for temperatures above that of the I-VII-fluid triple point (800 K), a sample of phase IV may be decompressed down to the melting line without transiting into phase VII [11]. A polycrystal of phase IV was thus prepared by annealing the sample at 15 GPa up to 830 K, and then slowly decompressed isothermally down to the melting point. At melting, the polycrystalline sample rapidly recrystallizes and a single crystal seed in equilibrium with its melt is eventually obtained (Fig. 2). The temperature was then slowly lowered down to ambient at constant *P*, as phase IV is known to be metastable at room temperature [7].

X-ray diffraction experiments were conducted at the European Synchrotron Radiation Facility (Grenoble, France) on beam lines ID09 and ID27. We used the angular dispersive technique with monochromatic x rays of wavelength ~0.4 Å and 2D detectors.

Figure 2(a) shows the diffraction pattern from the CO_2-IV crystal at 15.2 GPa, 295 K. The sharp diffraction spots testifies of its high quality. Analysis of the data suggested the two rhombohedral space groups $R3c$ and $R\bar{3}c$ as possible crystalline symmetries [13]. The cell parameters are $a_R = 6.108(1)$ Å and $\alpha_R = 89.87(5)°$ for the primitive rhombohedral cell, and $a_H = 8.628(1)$ Å, $c_H = 10.604(4)$ Å for the conventional *R*-centered cell (hexagonal axes) [14]. To match the estimated density at this pressure, the primitive (respectively, *R* centered) cell must contain 8 (respectively, 24) molecules. The structure was initially solved in space group $R3c$ using direct methods, but it turned out that the same solution could be refined in $R\bar{3}c$ with no loss in fit quality. The asymmetric unit of the $R\bar{3}c$ structure contains two pairs of carbon and oxygen atoms (C1, O1) and (C2, O2) which, by addition of the missing oxygen atoms generated by symmetry, form two symmetry inequivalent molecules $M1$ and $M2$. $M1$ lies along the threefold axis on a site of symmetry S_6, whereas $M2$ is oriented perpendicular to the twofold axis at $(0, y, \frac{1}{4})$ and occupies a site of symmetry C_2. After refinement of the atomic positions and anisotropic thermal parameters (20 parameters in total for 157 independent reflections), the residual factors R_1 and wR_2 decreased to 0.035 and 0.068, respectively, showing that the model fits the data very well. The final structural parameters, data collection, and refinement details are given in Table I and Ref. [15].

The C = O bond distance is, within standard deviations, the same for $M1$ and $M2$, 1.155(2) Å. This value takes into account the small correction (+0.005 Å) due to thermal vibration using the simple rigid bond model from Ref. [16]. For comparison, the C = O bond distance reported for phase I at 1 GPa, 295 K is 1.168 Å [17], which is the same as that determined in the gas phase [18]. The intramolecular bond thus *shortens* under pressure, in sharp opposition to the intermediate bonding scenario. Moreover, no bending of the molecules is observed: the <COC angles are 180(0)° and 179.8(2)° for $M1$ and $M2$, respectively. The present experiments thus corroborate the theoretical results of Bonev *et al.* [10] who showed that elongated and bent bonds are highly unstable in the *P*-*T* range of phases II and IV.

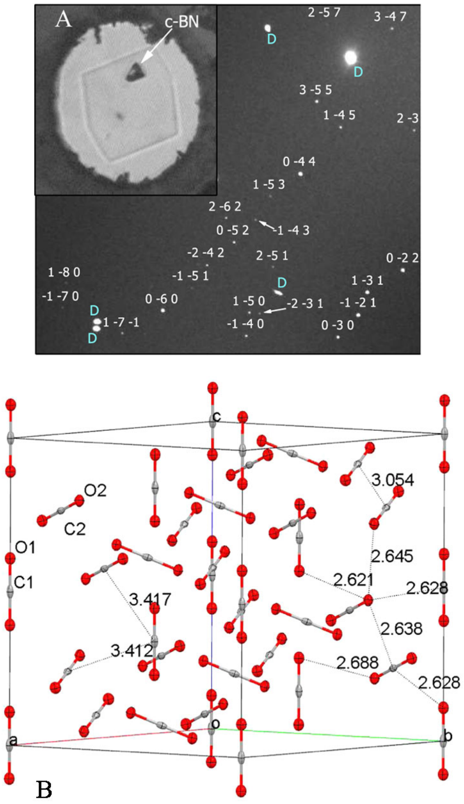

FIG. 2 (color online). (a) Detail of the diffraction pattern of a CO_2-IV single crystal at 15.2 GPa and 295 K, obtained by rotating the crystal by 60° around the ω axis. The numbers are (hkl) indices of reflections from the CO_2 crystal, while *D* indicates reflections from the diamond anvils. The inset shows a picture of the faceted single crystal in equilibrium with the fluid at 11.7 GPa–830 K, as viewed through the diamond anvils. The small *c*-BN crystal, shown by the arrow, is used to determine pressure. (b) Unit cell of CO_2-IV (hexagonal axes). Thermal ellipsoids are drawn at the 50% probability level. Selected intermolecular distances are indicated in Å.

Figure 2(b) shows a plot of the CO_2-IV structure. By contrast with other crystal structures of molecular CO_2, phase IV is not a layer-type structure. Still, it shows some similarities with the $Pa\bar{3}$ phase I as illustrated in Fig. 3: looking at the first neighbor shell of molecules around $M1$, the biggest difference between the two structures is that the

TABLE I. Refined structural parameters of the $R\bar{3}c$ structure at 15.2 GPa and 295 K. See also Ref. [15].

Unit cell (hex. axis)			$a_H = 8.628(1)$ Å	$c_H = 10.604(4)$ Å
Label	x	y	z	$U_{\text{iso/equiv}}$
C1	0	0	0	0.0116
O1	0	0	0.1084(2)	0.0148
C2	0	0.2499(2)	0.25	0.0095
O2	0.1418(1)	0.3205(1)	0.2077(1)	0.0143

six molecules having the C atom sitting on the same plane as the central one in $Pa\bar{3}$, have shifted either up or down from this plane in $R\bar{3}c$, resulting in a more compact structure. This resemblance, however, no longer holds at farther distances.

The shortest intermolecular distances at 15.2 GPa are indicated in Fig. 2(b). Each C atom has six nearest O atoms on neighbor molecules distributed in the narrow shell 2.6275(5)–2.6679(4) Å. The intermolecular C-O distance has shrunk by ~13% with respect to its value at 1 GPa (the volume has reduced by 31%) but remains more than twice as large as the intramolecular one. C1 atoms are surrounded by 12 C2 atoms at 3.415 ± 0.003 Å in the first neighbor shell, similarly as in phase I, but the shortest intermolecular C-C distance are between C2 atoms in slipped parallel configuration at 3.0541(4) Å.

Diffraction data from the same crystal were also collected after increasing pressure to 18.3 GPa, corresponding to a volume reduction of 3.6%. We repeated the refinement in $R\bar{3}c$ and obtained very similar fit quality and results as for the lower pressure (see Ref. [15]). In particular, the $C = O$ bond length has not changed. To check that this structure is the same at high temperature, we performed a second run where a new crystal was grown and diffraction data collected at 15.9 GPa and 638 K. The quality of this data set is significantly lower than the two previous ones; however, the refinement in the $R\bar{3}c$ structure is stable: the values found for the $C = O$ bond length [1.16(1) Å] and <COC angles [180(1)° for $M2$] are consistent with those obtained at ambient temperature [15].

It is noteworthy that the $R\bar{3}c$ structure has never been predicted nor considered by reported theoretical studies as a possible polymorph for molecular CO_2. We report here calculations based on density functional theory (DFT) using either the local-density (LDA) or generalized-gradient [19] (GGA) approximations [20]. We started from the experimental unit cell and optimized all structural parameters at several volumes. The structure is found stable and the final atomic positions are very close to experimental ones [15]. The $C = O$ bond length determined at the measured volume at 15.2 GPa is larger than the experimental one (1.163 Å and 1.167 Å for LDA and GGA, respectively), but is also found to decrease with pressure, at a rate of about -0.0004 Å/GPa. We also note that the theoretical bond length previously determined [10] for the $P4_2/mnmn$ phase II, 1.154 Å, is in excellent agreement with present findings. The experimental volume of $R\bar{3}c$ is bracketed by the LDA and GGA results, as frequently observed, although GGA provides a closer match. The bulk modulus B_0 and its first pressure derivative B_0' at $P = 0$, obtained by fitting a third-order Birch-Murnaghan form [22], are $B_0 = 2.5(2)$ GPa and $B_0' = 7.9(2)$ for GGA, and $B_0 = 10.7(1)$ GPa and $B_0' = 7.06(3)$ for LDA. These values are very similar to those found for other molecular phases of CO_2 [10], and typical of molecular solids.

The theoretical Raman spectrum of the $R\bar{3}c$ structure was computed via density functional perturbation theory [23] in the GGA approximation, and is compared to the experimental one in Fig. 4 (for clarity, the spectra have been truncated to frequencies below 700 cm^{-1}). Using group theory, it can be shown that the $R\bar{3}c$ structure has 9 Raman (R) + 9 infrared (IR) active lattice modes, $3R$ + 1IR active ν_1 modes, $3R$ + 4IR active ν_2 modes and $1R$ + 3IR active ν_3 modes. There is a remarkable agreement between calculated and measured Raman spectra, especially for the lattice modes. The ~8% frequency difference for the ν_2 (bending) modes is of similar amplitude as that obtained for the isolated molecule: in this case, DFT calculations give 630 cm^{-1}, while experiment gives 668 cm^{-1}. The five most intense lattice peaks of the theoretical IR spectra at 20 GPa (equivalent to an experimental pressure of ~17 GPa) are at 86, 191.1, 211.5, 237.7, and 262.5 cm^{-1}, here again in excellent correspondence with experiment [8].

It is striking that the $R\bar{3}c$ structure is also adopted by N_2 and CO molecules at high pressure [24]. CO_2 and N_2 further share the $Pa\bar{3}$ and $P4_2/mnm$ structures at lower P/T conditions, making their phase diagrams quite similar as far as the molecular phases are concerned. Ignoring thermal effects—responsible for the presence of orientationally disordered δ and β phases in N_2 at high T—the phase diagram up to ~30 GPa of these rod-shaped molecules may be rationalized in terms of competing effects between the electric quadrupole-quadrupole (EQQ) interactions and compactness. The $Pa\bar{3}$ structure is known to minimize the EQQ interactions which dominate at low density, while the $Pa\bar{3} \rightarrow P4_2/mnm$ transition was shown to be driven in N_2 by the more efficient packing of the dumbbell-like molecules [25]. The similarity between the $Pa\bar{3}$ and $R\bar{3}c$ structures outlined above suggests that the

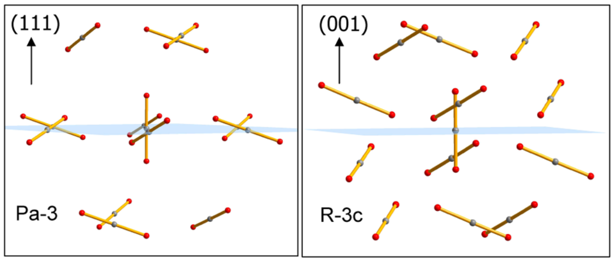

FIG. 3 (color online). Comparison between the $Pa\bar{3}$ phase I and $R\bar{3}c$ phase IV structures, looking at the first neighbor shell of molecules around a molecule of type $M1$.

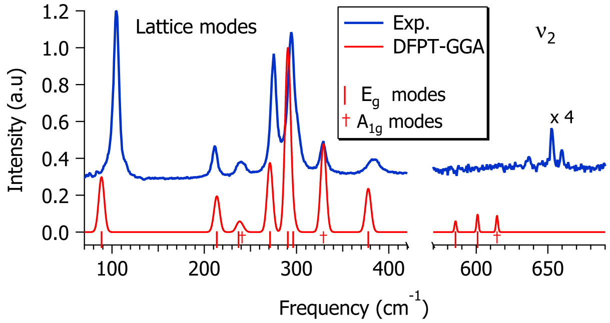

FIG. 4 (color online). Comparison between the experimental Raman spectrum of phase IV (top blue curve), and the theoretical one of $R\bar{3}c$(bottom red curve). The former was measured at 20.9 GPa and 295 K on the same sample as that used for the x-ray diffraction experiment at 295 K, from which the crystal structure was solved. The theoretical spectrum was computed at the same volume as the experimental one. An arbitrary width has been added to the peaks for easier visualization (3 and 0.7 cm^{-1} for lattice and ν_2 modes respectively). Symbols indicate calculated frequencies for E_g (|) and A_{1g} (†) modes.

influence of the EQQ interactions persists in the latter structure, although constrained by a denser arrangement of the molecules.

In conclusion, we have determined the crystalline structure of CO_2-IV to be rhombohedral, space group $R\bar{3}c$. This structure is composed of linear molecules with a $C = O$ bond length slightly smaller than that of the isolated molecule. This result invalidates the intermediate bonding state scenario and thus supports the idea that polymerization occurs via solid-state chemical reactions between CO_2 molecules. The present findings are not only important to rationalize the phase diagram of molecular CO_2, but are also highly relevant for our understanding of the formation of polymeric phases; indeed, recent studies show that the final polymeric phase strongly depends on the starting molecular structure [4,5,26]. In particular, the structure of polymeric phase V, which is still debated [3], could well be related to that of phase IV, as Yoo *et al.* reported direct forward and backward transitions between IV and V by heating above or below 30 GPa, respectively [27].

We acknowledge the ESRF for provision of beam time under proposals HS3392 and HD226. We wish to thank M. Merlini and M. Mezouar for their valuable help. Theoretical calculations were performed at IDRIS supercomputing facility under projects CP9-81387 and CP9-91387.

---

[1] V. Iota, C. S. Yoo, and H. Cynn, Science **283**, 1510 (1999).
[2] C. S. Yoo, H. Cynn, F. Gygi, G. Galli, V. Iota, M. Nicol, S. Carlson, D. Häusermann, and C. Mailhiot, Phys. Rev. Lett. **83**, 5527 (1999).
[3] M. Santoro and F. A. Gorelli, Chem. Soc. Rev. **35**, 918 (2006).
[4] M. Santoro, R. B. G. R. Federico, A. Gorelli, S. Scandolo, and W. A. Crichton, Nature (London) **441**, 857 (2006).
[5] V. Iota, C. S. Yoo, J. H. Klepheis, Z. Jenei, W. Evans, and H. Cynn, Nature Mater. **6**, 34 (2007).
[6] J. A. Montoya, R. Rousseau, M. Santoro, F. Gorelli, and S. Scandolo, Phys. Rev. Lett. **100**, 163002 (2008).
[7] J. H. Park, C. S. Yoo, V. Iota, H. Cynn, M. F. Nicol, and T. Le Bihan, Phys. Rev. B **68**, 014107 (2003).
[8] F. A. Gorelli, V. M. Giordano, P. R. Salvi, and R. Bini, Phys. Rev. Lett. **93**, 205503 (2004).
[9] C. S. Yoo, H. Kohlmann, H. Cynn, M. F. Nicol, V. Iota, and T. Le Bihan, Phys. Rev. B **65**, 104103 (2002).
[10] S. A. Bonev, F. Gygi, T. Ogitsu, and G. Galli, Phys. Rev. Lett. **91**, 065501 (2003).
[11] V. M. Giordano and F. Datchi, Europhys. Lett. **77**, 46002 (2007).
[12] V. M. Giordano, F. Datchi, and A. Dewaele, J. Chem. Phys. **125**, 054504 (2006).
[13] Data reduction of the diffraction images was performed using the CRYSALISPRO [Oxford Diffraction LTD., Version 1.171.31 (2009)] or XDS [W. Klabsch, J. Appl. Crystallogr. **26**, 795 (1993)] softwares. Structure solution and refinements were done with the SIR2004 [M. Burla, R. Caliandro, M. Camalli, B. Carrozzini, G. Cascarano, L. D. Caro, C. Giacovazzo, G. Polidori, and R. Spagna, J. Appl. Crystallogr. **38**, 381 (2005)] and Crystals [P. W. Betteridge, J. R. Carruthers, R. I. Cooper, K. Prout, and D. J. Watkin, J. Appl. Crystallogr. **36**, 1487 (2003)] programs, respectively.
[14] Estimated standard deviations are indicated in parentheses.
[15] See EPAPS Document No. E-PRLTAO-103-034946 for auxiliary tables. For more information on EPAPS, see http://www.aip.org/pubservs/epaps.html.
[16] R. T. Downs, G. V. Gibbs, K. L. Bartelmehs, and M. B. Boisen, Am. Mineral. **77**, 751 (1992).
[17] R. T. Downs and M. S. Somayazulu, Acta Crystallogr. Sect. C **54**, 897 (1998).
[18] I. Karle and J. Karle, J. Chem. Phys. **17**, 1052 (1949).
[19] J. P. Perdew, K. Burke, and M. Ernzerhof, Phys. Rev. Lett. **77**, 3865 (1996).
[20] We used the PWSCF and PHONON codes included in the QUANTUM ESPRESSO distribution [21], adopting a plane wave and pseudopotential approach. Carbon and oxygen were described through ultrasoft pseudopotentials, which allowed a kinetic energy cutoff of 30 Ry. Brillouin zone sampling was obtained with uniform $4 \times 4 \times 4$ grids.
[21] S. Baroni *et al.*, http://www.quantum-espresso.org.
[22] F. Birch, J. Geophys. Res. **83**, 1257 (1978).
[23] S. Baroni, S. de Gironcoli, A. D. Corso, and P. Giannozzi, Rev. Mod. Phys. **73**, 515 (2001).
[24] R. L. Mills, B. Olinger, and D. T. Cromer, J. Chem. Phys. **84**, 2837 (1986).
[25] J. C. Raich and R. L. Mills, J. Chem. Phys. **55**, 1817 (1971).
[26] J. Sun, D. D. Klug, R. Martoňák, J. A. Montoya, M.-S. Lee, S. Scandolo, and E. Tosatti, Proc. Natl. Acad. Sci. U.S.A. **106**, 6077 (2009).
[27] C. S. Yoo, V. Iota, and H. Cynn, Phys. Rev. Lett. **86**, 444 (2001).